Applied Physics Letters ARTICLE scitation.org/journal/apl

Sub-2 cm/s passivation of silicon surfaces by aprotic solutions

Cite as: Appl. Phys. Lett. **116**, 121601 (2020); doi: 10.1063/5.0003704
Submitted: 4 February 2020 · Accepted: 10 March 2020 ·
Published Online: 25 March 2020

Alex I. Pointon,[1] Nicholas E. Grant,[1] Sophie L. Pain,[1] Joshua T. White,[2] and John D. Murphy[1,a)]

AFFILIATIONS

[1]School of Engineering, University of Warwick, Coventry CV4 7AL, United Kingdom
[2]Department of Chemistry, University of Warwick, Coventry CV4 7AL, United Kingdom

[a)]Author to whom correspondence should be addressed: john.d.murphy@warwick.ac.uk

ABSTRACT

Minimizing recombination at semiconductor surfaces is required for the accurate determination of the bulk carrier lifetime. Proton donors, such as hydrofluoric acid and superacids, are well known to provide highly effective short-term surface passivation. We demonstrate here that aprotic solutions based on bis(trifluoromethanesulfonyl)methane (TFSM) in hexane or pentane can also result in excellent passivation of (100)-orientation silicon surfaces. We show that the optimized TFSM-pentane passivation scheme can measure effective lifetimes up to 20 ms, with a surface recombination velocity of 1.7 cm s^{-1} at an excess carrier density of 10^{15} cm^{-3}. Fitting injection-dependent lifetime curves requires chemical passivation and field effect passivation from a negatively charged layer with a charge density of 10^{10}–10^{11} q cm^{-2}. The slightly higher recombination velocity of 2.3 cm s^{-1} measured with TFSM-hexane can be explained by a lower charge density in the passivating layer, suggesting that the steric hindrance associated with the solvent size could play a role in the passivation mechanism. Finally, phosphorus nuclear magnetic resonance experiments confirm that TFSM-based solutions have Lewis acidity without being superacids, which opens up opportunities for them to be used in materials systems sensitive to superacidic environments.

The efficient operation of many silicon-based microelectronic and photovoltaic devices is contingent on achieving a high bulk excess carrier lifetime and maintaining this during device processing. The measurement of high effective lifetimes requires suppression of surface recombination. Dielectrics are frequently used for surface passivation, including silicon nitride (SiN_x), aluminum oxide (Al_2O_3), and amorphous silicon (a-Si).[1] Unfortunately, their deposition or subsequent annealing can change the bulk lifetime of the material. This can be because hydrogen is introduced into the bulk from the dielectric,[2] bulk recombination centers are formed or annihilated depending on the annealing temperature,[3] or impurities from the bulk are gettered to the dielectric layer.[4] This means that dielectric-based passivation is often unsuitable for determining the true bulk lifetime of a silicon wafer.

Room temperature temporary passivation schemes (see Ref. 5 for a review) do not generally modify the bulk lifetime under investigation and so are valuable in the evaluation of the effect of device processing steps and in providing consistent bulk lifetime values for device simulations. For (100)-orientation silicon surfaces, the most successful temporary passivation schemes rely on proton donors and include hydrofluoric (HF) acid immersion[6,7] and surface treatments with superacidic solutions.[8–11] These schemes can provide a surface recombination velocity, S, below 1 cm s^{-1}.[6,9,10] Non-acidic methods, such as halogen-alcohols, typically give best-case S values of 5–10 cm s^{-1}.[12–14]

Our recent work has shown that a whole class of chemicals with a bis(trifluoromethanesulfonyl)-based structure can passivate silicon surfaces.[11] While this includes the superacid bis(trifluoromethane)sulfonimide (TFSI), other chemicals in this family are not superacidic or even proton donors. The current paper demonstrates that aprotic chemicals (i.e., those which do not donate protons) can also give excellent passivation of silicon surfaces, at a level better than halogen-alcohols, and approaching that of proton donors such as HF and superacids. This is important because there are intrinsic hazards associated with the use of HF and, while superacids are compatible with silicon, their strong acidity prevents their use on more sensitive electronic materials.

We focus here on a molecule called bis(trifluoromethanesulfonyl)methane (TFSM), which is shown in Fig. 1(a). This has a very similar structure to the TFSI superacid, with a CH_2 group in TFSM replacing the central NH group in the TFSI. The single hydrogen in the TFSI central group is highly labile, and when TFSI crystals are

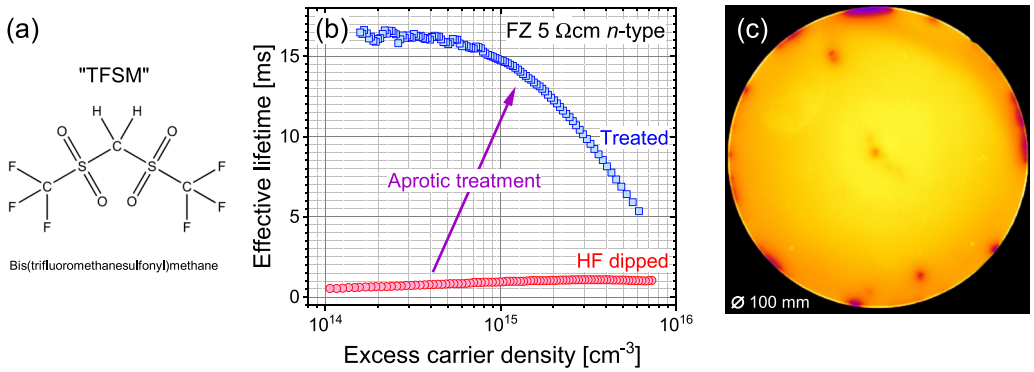

FIG. 1. (a) Schematic of the bis(trifluoromethanesulfonyl)methane (TFSM) molecule. (b) Effective excess carrier lifetime measured in a 700 μm thick 5 Ωcm *n*-type FZ silicon wafer after an HF dip and after a TFSM-pentane treatment. (c) Uncalibrated PL image of a 100 mm diameter wafer treated with the TFSM-pentane passivation scheme, showing the high process uniformity across the wafer surface.

dissolved in an appropriate solvent, a very strong superacidic solution is formed, which contains a highly electronegative $(CF_3SO_2)_2N$ species.[15] In TFSM, the central hydrogens are strongly bound to the carbon atom and the solution that is formed when the crystal is dissolved is aprotic. In this paper, we first show that TFSM-based treatments can give excellent passivation of silicon surfaces. We show that the passivation is weakly dependent on the choice of solvent, and we then use a robust method based on variable thickness wafers from the same ingot to measure the surface recombination velocity. Finally, we model the lifetime data obtained as a function of excess carrier density in order to quantify surface charge and the relative change in interface trap density resulting from the treatment.

All experiments were performed on float-zone (FZ) *n*-type (100)-orientation silicon wafers. Measurements were made on either 700 μm thick 5 Ω cm 100 mm diameter wafers or four 3 Ω cm wafers of different thicknesses (initially 250–1500 μm) cut from the same ingot. Samples were subjected to a rigorous pre-cleaning and surface preparation procedure described previously.[10] The varying thickness wafer set was re-used with an additional Standard Clean 1 (SC1) procedure using de-ionized water H_2O, ammonium hydroxide NH_4OH (30%), and hydrogen peroxide H_2O_2 (30%) in the ratio 5:1:1 for 10 min at ∼80 °C first performed to remove residual solvent contamination. Passivating solutions were made from 100 mg of bis(trifluoromethane)sulfonimide (TFSI) (>95% purity) or bis(trifluoromethanesulfonyl)methane (TFSM) (>97% purity) in 200 ml of anhydrous hexane (>95% purity) or anhydrous pentane (≥99% purity) and were prepared in gloveboxes as described previously.[11] All chemicals were purchased from Sigma-Aldrich. The passivation treatment was performed by dipping the prepared samples into solutions inside a N_2 ambient glovebox (relative humidity ∼25%). Samples were immersed for 1 min before being removed and allowed to dry. Transient photoconductance decay effective carrier lifetime measurements were made using a Sinton WCT-120 system. Calibration of lifetime measurements for the very thick samples was accounted for using the method of Black and Macdonald described in Ref. 16. Lifetime measurements are assumed to be accurate to ± 4% (guided by Blum *et al.*[17]). The spatial uniformity of the passivation treatment was determined by photoluminescence (PL) imaging[18] using a BT Imaging LIS-L1 PL imaging tool with a photon flux of $2.55 \times 10^{17}\,cm^{-2}\,s^{-1}$ and an exposure time of 0.1 s.

While TFSM solutions are aprotic (they do not donate protons), they do exhibit Lewis acidity as they are able to accept electron pairs. To quantify Lewis acidity, we use the Gutmann–Beckett method based on ^{31}P NMR in which our chemical of interest is dissolved with triethylphosphine oxide (TPO) in a deuterated solvent.[19,20] The Lewis acid interacts with the basic oxygen in the TPO, which has the effect of deshielding the phosphorus center in the TPO. The resulting shift in the ^{31}P NMR spectrum can be used to quantify the acceptor number from the peak shift in ppm, δ_{peak}, as[20]

$$AN = 2.21 \times (\delta_{peak} - 41.0), \quad (1)$$

which is a quantitative measurement of Lewis acidity. For our studies, we took TFSI or TFSM and TPO (97% purity, Sigma-Aldrich) at the ratio of 3:1–4:1 by mass to ensure the complete formation of the TPO-acid adduct[21] and dissolved this in deuterated chloroform (>99.8% purity with 0.03% tetramethylsilane from Apollo Scientific). We collected $^{31}P\{^1H\}$ (proton decoupled) NMR spectra using a Bruker Avance III HD 300 MHz system by averaging over 64 scans at room temperature. The NMR spectrometer had been calibrated to an 85% H_3PO_4 reference ($\delta = 0$). Table I shows the average NMR peak shift for TPO, TPO in the presence of TFSM (TFSM-TPO) and TPO in the presence of TFSI (TFSI-TPO). The determined TPO acceptor number of 25.2 in deuterated chloroform is similar to the literature value of 23.1 in (non-deuterated) chloroform.[19] TFSI-TPO has an acceptor number of 116.3, which is consistent with its known superacidic properties. We are not aware of previous measurements of the acceptor number for TFSI in the literature, but we note that our measurement for TFSI [which has formula $(CF_3SO_2)_2NH$] is similar to that (129.1)

TABLE I. Average peak shift from $^{31}P\{^1H\}$ NMR experiments on various compounds dissolved in deuterated chloroform. The acceptor number, *AN*, is calculated using Eq. (1).

Compound	Average δ_{peak} (ppm)	AN
TPO only	52.4	25.2
TFSM-TPO	73.0	70.7
TFSI-TPO	93.6	116.3

for trifluoromethanesulfonic acid (CF_3SO_2OH) that also has a CF_3SO_2 unit.[22] TFSM-TPO has a lower acceptor number of 70.7, which confirms that it is a moderate Lewis acid, without being superacidic.

Figure 1(b) shows the effect of a TFSM-pentane treatment on the effective lifetime of a 700 μm thick 5 Ω cm n-type silicon sample. This aprotic treatment increases the effective lifetime from the HF dipped state substantially, with lifetimes in excess of 16 ms measured at low injection. At an excess carrier density of 10^{15} cm^{-3}, the effective lifetime after the HF dip was 0.94 ms, which shows that the hydrogen termination of the surface provides some passivation, and this increased to 14.7 ms after the TFSM-treatment. As with TFSI-based passivation,[8–11] TFSM-based passivation degrades with time in air; however, the passivation is sufficiently stable for reliable characterization of silicon wafers with high lifetimes. The spatial uniformity of TFSM-pentane passivation is shown in the PL image of a whole 100 mm diameter wafer in Fig. 1(c). There is a high and uniform PL signal across the whole wafer, with the small darker sections around the perimeter of the wafer likely to arise from wafer handling damage during processing and characterization.

A series of experiments was performed to characterize the aprotic TFSM-based passivation treatments in terms of the surface recombination velocity, S. For symmetrically passivated wafers, the effective lifetime, $\tau_{effective}$, varies according to

$$\frac{1}{\tau_{effective}} = \frac{1}{\tau_{bulk}} + \frac{2S}{W}, \quad (2)$$

where τ_{bulk} is the bulk lifetime of the material, W is the wafer thickness, and S is the surface recombination velocity. $\tau_{effective}$, τ_{bulk}, and S vary with excess carrier density. In many studies, an upper limit of S is determined by taking τ_{bulk} as infinity. A better methodology is to take wafers with the same τ_{bulk} cut to different thicknesses, as this enables the measurement of an absolute value of S, and this is the approach we have taken.

The lifetime results for different thickness wafers cut from the same ingot (hence assumed to have the same bulk lifetime) are shown in Fig. 2(a) for TFSM-hexane passivation and in Fig. 2(b) for TFSM-pentane passivation. In both cases, the lifetime increases with the wafer thickness as the contribution of surface recombination relative to bulk recombination decreases. The same wafers were used for both passivation schemes, and hence, the thicknesses in Fig. 2(b) are slightly less than those in Fig. 2(a) as the wafers are etched during surface preparation. Equation (2) was used at each excess carrier density at which all lifetime curves were available to calculate the bulk lifetime, and this is also plotted on the graphs. The bulk lifetimes are consistent within error, which is to be expected as they are deduced from a common sample set. The intrinsic lifetime limit from the study by Richter *et al.*[23] is shown on the graphs. The bulk lifetime exceeds the so-called limit at higher levels of injection, which is consistent with other recent studies[9,24,25] and shows that the intrinsic limit parameterization is in need of minor revision.

Figure 3(a) shows a plot in accordance with Eq. (2) used to extract the surface recombination velocity and bulk lifetime at an excess carrier density of 10^{15} cm^{-3}. Data are shown for three different passivation schemes, with TFSM-hexane and TFSM-pentane being aprotic, and TFSI-hexane being superacidic. The three passivation schemes give a consistent bulk lifetime of around 35 ms. The surface recombination velocity is around 0.7 cm s^{-1} for TFSI-hexane, which is as expected from our previous work.[10] The aprotic passivation schemes have higher surface recombination velocities of around 1.7 cm s^{-1} for TFSM-pentane and 2.3 cm s^{-1} for TFSM-hexane. Figure 3(b) shows the dependence of surface recombination velocity on excess carrier density. The surface recombination velocity generally increases with excess carrier density, in agreement with other passivation schemes such as iodine–ethanol[14] and Al_2O_3.[26]

It is clear from the results in Fig. 3 that the choice of solvent for TFSM affects the level of surface passivation achieved, with better passivation achieved with anhydrous pentane (C_5H_{12}, molar mass: 72.15 g mol^{-1}) than with anhydrous hexane (C_6H_{14}, molar mass: 86.18 g mol^{-1}). Similar solvent-related effects have been measured with TFSI-based passivation previously, with octane (C_8H_{18}) giving much worse passivation than hexane.[10] Steric effects associated with larger solvent molecules, therefore, appear to affect the passivation quality. An alternative explanation is that impurities in the solvent affect the passivation achieved, as we note that the specified purity limit of hexane is lower than that of pentane.

More insight into the passivation mechanisms can be gained from fitting injection-dependent lifetime curves. In general, surface

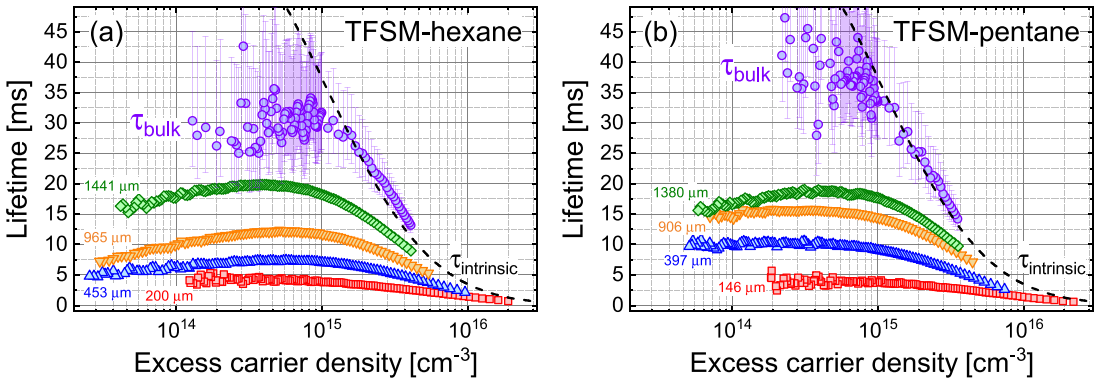

FIG. 2. Effective carrier lifetime measured on four 100 mm diameter 3 Ωcm n-type FZ silicon wafers with different thicknesses, which were passivated using (a) a TFSM-hexane treatment and (b) a TFSM-pentane treatment. Equation (2) is applied at each excess carrier density at which there are data for all four samples to extract the bulk lifetime. The intrinsic lifetime parameterisation from the study by Richter *et al.*[23] is shown as a dashed line.

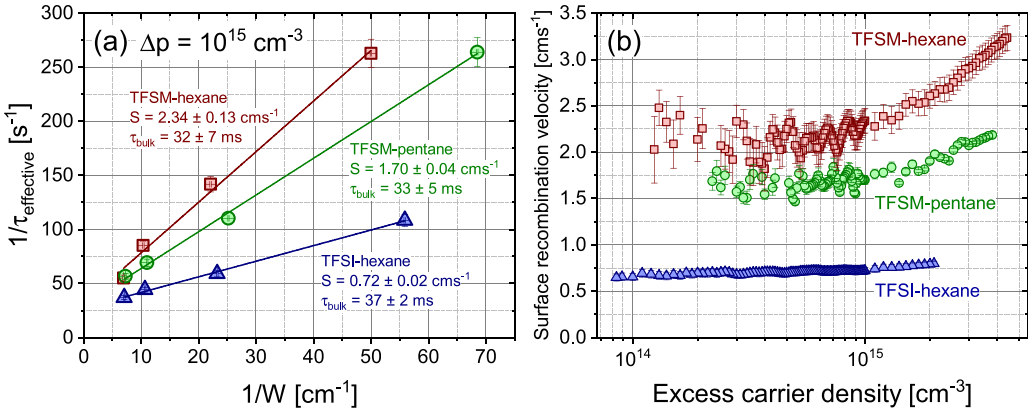

FIG. 3. (a) A plot in accordance with Eq. (2) used to extract the surface recombination velocity, S, and the bulk lifetime, τ_{bulk}, from 3 Ω cm n-type FZ silicon wafers at an excess carrier density, Δp, of 10^{15} cm^{-3} for different passivation schemes. (b) Extracted S as a function of excess carrier density.

passivation is determined by a combination of chemical and field effects, governed by the interface state density (D_{it}) and effective areal charge density (Q_{eff}), respectively. Figure 4 shows the results of the fitting of the lifetime curves that are taken for the 3 Ωcm n-type sample which is approximately 400 μm thick from Fig. 2, treated with TFSM-hexane and TFSM-pentane. We model the lifetime curves using a method described by Girisch *et al.*[27] and extended by Aberle *et al.*[28] using software available from PV Lighthouse,[29] assuming that the surface recombination is governed by a single defect at mid-gap. We account for intrinsic recombination using the parameterization from the study by Richter *et al.*[23] Fitting both effective lifetime curves requires the inclusion of negative charge in the passivating layer, which is to be expected given our previous Kelvin probe data for TFSI-hexane samples.[11] We model the chemical passivation in terms of a carrier type-specific surface recombination parameter, which for electrons is $S_{n0} = \nu_{tn} \times \sigma_n \times D_{it}$ and for holes is $S_{p0} = \nu_{tp} \times \sigma_p \times D_{it}$, where ν_{tn} is the thermal velocity of electrons, ν_{tp} is the thermal velocity of holes, and σ_n and σ_p are the capture cross sections for electrons and holes, respectively. From lifetime data alone, it is not possible to separate the cross section and interface state density terms. The parameters used to fit the curves are shown in Fig. 4. Our fits are relatively insensitive to S_{p0} and require a slightly larger S_{n0} for TFSM-pentane than TFSM-hexane. The mechanism of the passivation, therefore, appears to be similar to superacidic passivation,[11] insofar as some of the passivation arises from the hydrogen termination after the final HF dip stage and the additional TFSM-based treatment adds negative charge to the surface.

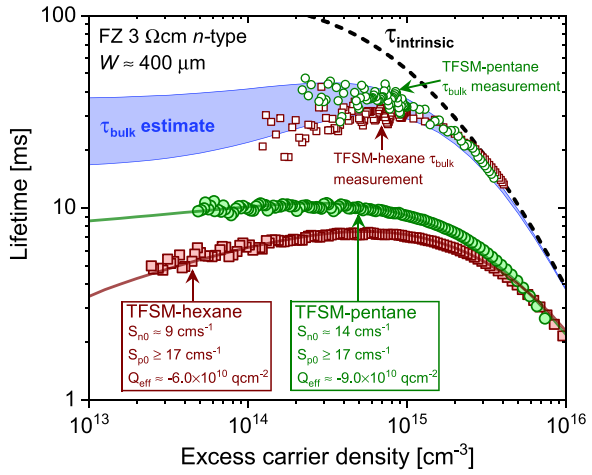

FIG. 4. Fitting of injection-dependent lifetime curves for 3 Ω cm n-type FZ silicon passivated with TFSM-pentane and TFSM-hexane using an approach described in the text. The extracted bulk lifetimes are also plotted, and an estimate of the bulk lifetime at lower injection is shown. The intrinsic lifetime parameterisation from the study by Richter *et al.*[23] is shown as a dashed line.

The results in this paper show that aprotic TFSM-based solutions provide excellent levels of surface passivation for (100)-orientation silicon surfaces, with surface recombination velocities < 2 cm s^{-1} measured with TFSM-pentane. This class of passivation is, therefore, considerably better than other temporary passivation schemes, such as iodine–ethanol, which can give $10 < S < 5$ cm s^{-1}.[12–14] Proton donating passivation schemes (e.g., HF, superacids) are established to give slightly better levels of surface passivation, but are likely to be more hazardous to use. Electronic materials that are less acid-resistant than silicon can benefit from surface passivation treatments (e.g., perovskite solar cells[30]), and, as we have established that aprotic solutions can also passivate, future work should focus on whether they also passivate more delicate materials systems.

This work was supported by the EPSRC SuperSilicon PV Project (No. EP/M024911/1), the EPSRC Impact Acceleration Account (No. EP/R511808/1), and an EPSRC First Grant (No. EP/J01768X/2). EPSRC studentship funding was received by A.I.P. (No. EP/N509796/1), S.L.P. (No. EP/R513374/1), and J.T.W. (No. EP/L015307/1). Sune Bro Duun of Topsil Semiconductor Materials is gratefully acknowledged for provision of the FZ-Si wafers with variable thicknesses from the same ingot.

Data underpinning figures in this paper can be downloaded from https://wrap.warwick.ac.uk/134280/. Requests for additional data should be made directly to the corresponding author.

REFERENCES

[1]R. S. Bonilla, B. Hoex, P. Hamer, and P. R. Wilshaw, "Dielectric surface passivation for silicon solar cells: A review," Phys. Status Solidi A **214**, 1700293 (2017).

[2]S. Wilking, S. Ebert, A. Herguth, and G. Hahn, "Influence of hydrogen effusion from hydrogenated silicon nitride layers on the regeneration of boron-oxygen related defects in crystalline silicon," J. Appl. Phys. **114**, 194512 (2013).

[3]N. E. Grant, V. P. Markevich, J. Mullins, A. R. Peaker, F. Rougieux, D. Macdonald, and J. D. Murphy, "Permanent annihilation of thermally activated defects which limit the lifetime of float-zone silicon," Phys. Status Solidi A **213**, 2844 (2016).

[4]A. Y. Liu, C. Sun, V. P. Markevich, A. R. Peaker, J. D. Murphy, and D. Macdonald, "Gettering of interstitial iron in silicon by plasma-enhanced chemical vapour deposited silicon nitride films," J. Appl. Phys. **120**, 193103 (2016).

[5]N. E. Grant and J. D. Murphy, "Temporary surface passivation for characterisation of bulk defects in silicon: A review," Phys. Status Solidi RRL **11**, 1700243 (2017).

[6]E. Yablonovitch, D. L. Allara, C. C. Chang, T. Gmitter, and T. B. Bright, "Unusually low surface-recombination velocity on silicon and germanium surfaces," Phys. Rev. Lett. **57**, 249 (1986).

[7]N. E. Grant, K. R. McIntosh, and J. T. Tan, "Evaluation of the bulk lifetime of silicon wafers by immersion in hydrofluoric acid and illumination," ECS J. Solid State Sci. Technol. **1**, P55 (2012).

[8]J. Bullock, D. Kiriya, N. Grant, A. Azcatl, M. Hettick, T. Kho, P. Phang, H. C. Sio, D. Yan, D. Macdonald, M. A. Quevedo-Lopez, R. M. Wallace, A. Cuevas, and A. Javey, "Superacid passivation of crystalline silicon surfaces," ACS Appl. Mater. Interfaces **8**, 24205 (2016).

[9]N. E. Grant, T. Niewelt, N. R. Wilson, E. C. Wheeler-Jones, J. Bullock, M. Al-Amin, M. C. Schubert, A. C. van Veen, A. Javey, and J. D. Murphy, "Superacid-treated silicon surfaces: Extending the limit of carrier lifetime for photovoltaic applications," IEEE J. Photovoltaics **7**, 1574 (2017).

[10]A. I. Pointon, N. E. Grant, E. C. Wheeler-Jones, P. P. Altermatt, and J. D. Murphy, "Superacid-derived surface passivation for measurement of ultra-long lifetimes in silicon photovoltaic materials," Sol. Energy Mater. Sol. Cells **183**, 164 (2018).

[11]A. I. Pointon, N. E. Grant, R. S. Bonilla, E. C. Wheeler-Jones, M. Walker, P. R. Wilshaw, C. E. J. Dancer, and J. D. Murphy, "Exceptional surface passivation arising from bis(trifluoromethanesulfonyl)-based solutions," ACS Appl. Electron. Mater. **1**, 1322 (2019).

[12]T. S. Horányi, T. Pavelka, and P. Tüttö, "In situ bulk lifetime measurement on silicon with a chemically passivated surface," Appl. Surf. Sci. **63**, 306 (1993).

[13]J. Chen, L. Zhao, H. Diao, B. Yan, S. Zhou, Y. Tang, and W. Wang, "Surface passivation of silicon wafers by iodine-ethanol (I-E) for minority carrier lifetime measurements," Adv. Mater. Res. **652–654**, 901 (2013).

[14]M. Al-Amin, N. E. Grant, A. I. Pointon, and J. D. Murphy, "Iodine–ethanol surface passivation for measurement of millisecond carrier lifetimes in silicon wafers with different crystallographic orientations," Phys. Status Solidi A **216**, 1900257 (2019).

[15]J. Foropoulos, Jr. and D. D. DesMarteau, "Synthesis, properties, and reactions of bis((trifluoromethyl)sulfonyl) imide $(CF_3SO_2)_2NH$," Inorg. Chem. **23**, 3720 (1984).

[16]L. E. Black and D. H. Macdonald, "Accounting for the dependence of coil sensitivity on sample thickness and lift-off in inductively coupled photoconductance measurements," IEEE J. Photovoltaics **9**, 1563 (2019).

[17]A. L. Blum, J. S. Swirhun, R. A. Sinton, F. Yan, S. Herasimenka, T. Roth, K. Lauer, J. Haunschild, B. Lim, K. Bothe, Z. Hameiri, B. Seipel, R. Xiong, M. Dhamrin, and J. D. Murphy, "Inter-laboratory study of eddy-current measurement of excess-carrier recombination lifetime," IEEE J. Photovoltaics **4**, 525 (2014).

[18]T. Trupke, R. A. Bardos, M. C. Schubert, and W. Warta, "Photoluminescence imaging of silicon wafers," Appl. Phys. Lett. **89**, 044107 (2006).

[19]V. Gutmann, "Solvent effects on the reactivities of organometallic compounds," Coord. Chem. Rev. **18**, 225 (1976).

[20]M. A. Beckett, G. C. Strickland, J. R. Holland, and K. S. Varma, "A convenient N.M.R. method for the measurement of Lewis acidity at boron centres: Correlation of reaction rates of Lewis acid initiated epoxide polymerizations with Lewis acidity," Polymer **37**, 4629 (1996).

[21]G. C. Welch, L. Cabrera, P. A. Chase, E. Hollink, J. D. Masuda, P. Wei, and D. W. Stephan, "Tuning Lewis acidity using the reactivity of "frustrated Lewis pairs": Facile formation of phosphine-boranes and cationic phosphonium-boranes," Dalton Trans. **31**, 3407 (2007).

[22]U. Mayer, V. Gutmann, and W. Gerger, "The acceptor number—A quantitative empirical parameter for the electrophilic properties of solvents," Monatsh. Chem. **106**, 1235 (1975).

[23]A. Richter, S. W. Glunz, F. Werner, J. Schmidt, and A. Cuevas, "Improved quantitative description of Auger recombination in crystalline silicon," Phys. Rev. B **86**, 165202 (2012).

[24]B. A. Veith-Wolf and J. Schmidt, "Unexpectedly high minority-carrier lifetimes exceeding 20 ms measured on 1.4-Ω cm n-type silicon wafers," Phys. Status Solidi RRL **11**, 1700235 (2017).

[25]T. Niewelt, A. Richter, T. C. Kho, N. E. Grant, R. S. Bonilla, B. Steinhauser, J.-I. Polzin, F. Feldmann, M. Hermle, J. D. Murphy, S. P. Phang, W. Kwapil, and M. C. Schubert, "Taking monocrystalline silicon to the ultimate lifetime Limit," Sol. Energy Mater. Sol. Cells **185**, 252 (2018).

[26]K. R. McIntosh and L. E. Black, "On effective surface recombination parameters," J. Appl. Phys. **116**, 014503 (2014).

[27]R. B. M. Girisch, R. P. Mertens, and R. F. De Keersmaecker, "Determination of Si-SiO_2 interface recombination parameters using a gate-controlled point-junction diode under illumination," IEEE Trans. Electron Devices **35**, 203 (1988).

[28]A. G. Aberle, S. Glunz, and W. Warta, "Impact of illumination level and oxide parameters on Shockley–Read–Hall recombination at the Si-SiO_2 interface," J. Appl. Phys. **71**, 4422 (1992).

[29]See www.pvlighthouse.com.au for "Calculator Map" for information regarding modelling of surface and bulk recombination in silicon materials.

[30]Q. Jiang, Y. Zhao, X. Zhang, X. Yang, Y. Chen, Z. Chu, Q. Ye, X. Li, Z. Yin, and J. You, "Surface passivation of perovskite film for efficient solar cells," Nat. Photonics **13**, 460 (2019).